

## Ebolavirus $\Delta$ -Peptide Immunoadhesins Inhibit Marburgvirus and Ebolavirus Cell Entry<sup>∇</sup>

Sheli R. Radoshitzky,<sup>1,2</sup> Kelly L. Warfield,<sup>1,3</sup> Xiaoli Chi,<sup>1</sup> Lian Dong,<sup>1</sup> Krishna Kota,<sup>1</sup> Steven B. Bradfute,<sup>1</sup> Jacqueline D. Gearhart,<sup>1</sup> Cary Retterer,<sup>1</sup> Philip J. Kranzusch,<sup>2</sup> John N. Misasi,<sup>4</sup> Marc A. Hogenbirk,<sup>2,5</sup> Victoria Wahl-Jensen,<sup>6</sup> Viktor E. Volchkov,<sup>7</sup> James M. Cunningham,<sup>4</sup> Peter B. Jahrling,<sup>6</sup> M. Javad Aman,<sup>1,3</sup> Sina Bavari,<sup>1</sup> Michael Farzan,<sup>2</sup> and Jens H. Kuhn<sup>2,6,8\*</sup>

*U.S. Army Medical Research Institute of Infectious Diseases, Fort Detrick, Frederick, Maryland 21702<sup>1</sup>; New England Primate Research Center, Harvard Medical School, Southborough, Massachusetts 01772<sup>2</sup>; Integrated BioTherapeutics, Inc., Germantown, Maryland 20876<sup>3</sup>; Brigham and Women's Hospital, Harvard Medical School, Boston, Massachusetts 02115<sup>4</sup>; Eijkman Graduate School for Immunology and Infectious Disease, Universiteit Utrecht, The Netherlands<sup>5</sup>; Integrated Research Facility at Fort Detrick, National Institute of Allergy and Infectious Diseases, National Institutes of Health, Fort Detrick, Frederick, Maryland 21702<sup>6</sup>; INSERM U758, Claude Bernard Université de Lyon-1, Ecole Normale Supérieure de Lyon, Lyon, France<sup>7</sup>; and Department of Biology, Chemistry, and Pharmacy, Freie Universität Berlin, 14195 Berlin, Germany<sup>8</sup>*

Received 14 December 2010/Accepted 9 June 2011

**With the exception of Reston and Lloviu viruses, filoviruses (marburgviruses, ebolaviruses, and “cuevaviruses”) cause severe viral hemorrhagic fevers in humans. Filoviruses use a class I fusion protein, GP<sub>1,2</sub>, to bind to an unknown, but shared, cell surface receptor to initiate virus-cell fusion. In addition to GP<sub>1,2</sub>, ebolaviruses and cuevaviruses, but not marburgviruses, express two secreted glycoproteins, soluble GP (sGP) and small soluble GP (ssGP). All three glycoproteins have identical N termini that include the receptor-binding region (RBR) but differ in their C termini. We evaluated the effect of the secreted ebolavirus glycoproteins on marburgvirus and ebolavirus cell entry, using Fc-tagged recombinant proteins. Neither sGP-Fc nor ssGP-Fc bound to filovirus-permissive cells or inhibited GP<sub>1,2</sub>-mediated cell entry of pseudotyped retroviruses. Surprisingly, several Fc-tagged  $\Delta$ -peptides, which are small C-terminal cleavage products of sGP secreted by ebolavirus-infected cells, inhibited entry of retroviruses pseudotyped with Marburg virus GP<sub>1,2</sub>, as well as Marburg virus and Ebola virus infection in a dose-dependent manner and at low molarity despite absence of sequence similarity to filovirus RBRs. Fc-tagged  $\Delta$ -peptides from three ebolaviruses (Ebola virus, Sudan virus, and Tai Forest virus) inhibited GP<sub>1,2</sub>-mediated entry and infection of viruses comparably to or better than the Fc-tagged RBRs, whereas the  $\Delta$ -peptide-Fc of an ebolavirus nonpathogenic for humans (Reston virus) and that of an ebolavirus with lower lethality for humans (Bundibugyo virus) had little effect. These data indicate that  $\Delta$ -peptides are functional components of ebolavirus proteomes. They join cathepsins and integrins as novel modulators of filovirus cell entry, might play important roles in pathogenesis, and could be exploited for the synthesis of powerful new antivirals.**

Filoviruses (marburgviruses, ebolaviruses, and “cuevaviruses” [20]) cause viral hemorrhagic fevers in humans with high case fatality rates (19). The notable exceptions are Reston virus (RESTV), an ebolavirus that is nonpathogenic for humans but virulent in other primates and possibly domestic pigs (2, 34), and Lloviu virus, a cuevavirus possibly pathogenic for bats (20). Currently, filovirus infections can neither be treated by antivirals nor prevented by vaccines.

Filovirus cell entry is mediated by a class I fusion protein, the spike protein GP<sub>1,2</sub> (23, 50). Its precursor assembles as a trimer. Each of its monomers is cleaved by furin into ectodo-

main GP<sub>1</sub> and transmembrane GP<sub>2</sub> subunits, which remain connected through a disulfide bond (12, 49, 51). GP<sub>1</sub> mediates receptor binding (12, 39) via a distinct receptor-binding region (RBR) located within its amino terminus (8, 21, 23). The identity of the receptor remains unclear, but recent data suggest that at least marburgviruses and ebolaviruses bind a shared cell surface receptor (21, 29). Filovirus particles are translocated into acidified endosomal compartments after receptor engagement (14, 30, 60). GP<sub>1</sub> is then cleaved to a 19-kDa intermediate by cathepsins B and L (6, 8, 38, 41), proteases that are regulated by  $\alpha_5\beta_1$ -integrin (42). Subsequent conformational changes in GP<sub>2</sub> facilitate fusion of the viral and cellular membranes (13, 17, 23, 37, 57).

Marburgviruses and ebolaviruses cause similar diseases in primates (19). However, marburgvirus GP genes encode only GP<sub>1,2</sub> spike proteins (12), whereas ebolavirus and cuevavirus GP genes express three proteins from individual, partially

\* Corresponding author. Mailing address: Integrated Research Facility at Fort Detrick, National Institute of Allergy and Infectious Diseases, National Institutes of Health, B-8200 Research Plaza, Fort Detrick, Frederick, MD 21702. Phone: (301) 631-7245. Fax: (301) 619-5029. E-mail: kuhnjens@mail.nih.gov.

<sup>∇</sup> Published ahead of print on 22 June 2011.

overlapping open reading frames (ORFs): GP<sub>1,2</sub> and two secreted glycoproteins, soluble GP (sGP) and small soluble GP (ssGP) (33, 40, 48), whose functions are unknown. The sGP precursor forms a homodimer (3, 11, 53) in parallel orientation (11, 53), and each monomer is cleaved by furin at its C terminus, yielding the mature sGP dimer and a secreted peptide,  $\Delta$ -peptide (54). sGP shares its N-terminal  $\approx$ 295 amino acid residues with GP<sub>1,2</sub> and ssGP (40, 48) and was therefore suggested to serve as a neutralizing antibody decoy in the bloodstream (16). Ebolavirion-like particles, produced by coexpression of the ebolavirus matrix protein VP40 and GP<sub>1,2</sub>, activate human endothelial cells and induce a decrease in barrier function exacerbated by exposure to tumor necrosis factor alpha (TNF- $\alpha$ ). sGP induces a recovery of the barrier function, indicating that it might play an anti-inflammatory role (56). Thus far, only one study has specifically addressed  $\Delta$ -peptide (54).  $\Delta$ -Peptide is a highly posttranslationally modified peptide (predicted mass of  $\approx$ 4.7 kDa; actual mass of  $\approx$ 10 to 14 kDa) that is rapidly and efficiently cleaved from the sGP precursor expressed from plasmids *in vitro*. However, in contrast to mature sGP,  $\Delta$ -peptide is retained in producer cells for extended periods of time before being released into the cell culture supernatant, and the overall amount of secreted peptide is less than that of sGP (54). Until now,  $\Delta$ -peptide was thought to be a mere by-product of sGP maturation without obvious function (54, 56). The absence of  $\Delta$ -peptide antibodies and the difficulty to create recombinant viruses expressing tagged  $\Delta$ -peptides due to the GP gene organization with its three overlapping reading frames have thus far prevented the detection of  $\Delta$ -peptide in sera of infected cells or animals.

In analogy to published experiments with GP<sub>1</sub> (21), we examined the cell surface binding and filovirus entry-inhibitory properties of Fc-tagged sGP, ssGP, and  $\Delta$ -peptide. Here, we report that sGP-Fc and ssGP-Fc did not influence filovirus cell entry. However, the Fc-tagged  $\Delta$ -peptides of three ebolaviruses (Ebola virus [EBOV], Sudan virus [SUDV], and Tai Forest virus [TAFV]) specifically inhibited cell entry of retroviruses pseudotyped with Marburg virus (MARV) GP<sub>1,2</sub>, as well as infectious Ebola virus and Marburg virus, in a dose-dependent manner and at low molarity. In contrast, the Fc-tagged  $\Delta$ -peptide of an ebolavirus nonpathogenic for humans (Reston virus) and that of an ebolavirus with lower lethality for humans (Bundibugyo virus) did not have an obvious phenotype. Our finding that the functional peptides bind to filovirus-permissive, but not to filovirus-resistant cells, and the observation that they inhibit entry of both marburgviruses and ebolaviruses despite the fact that  $\Delta$ -peptides are not produced by marburgviruses indicates that they interfere with a pathway used by all filoviruses to gain entry into target cells.

## MATERIALS AND METHODS

**Cell culture.** African green monkey kidney epithelial (Vero E6) cells, human cervical adenocarcinoma epithelial-like (HeLa) cells, and human acute T-cell leukemia Jurkat E6-1 T lymphocytes were obtained from the ATCC (CRL-1586, CCL-2, and TIB-152, respectively). Human embryonic kidney (HEK) 293T cells (52) were originally obtained from Joseph Sodroski, Dana Farber Cancer Institute, Boston, MA. Adherent (Vero E6, HeLa, and HEK 293T) cells were maintained in Dulbecco's modified Eagle's medium (DMEM), and a suspension (Jurkat E6-1) of T lymphocytes was maintained in RPMI 1640 medium (Gibco-Invitrogen), at 37°C in a humidified atmosphere containing 5% CO<sub>2</sub>.

**Viruses and infection assays.** Experiments with infectious filoviruses were performed under biosafety level 4 conditions. In the case of Ebola virus, Vero E6 cells were preincubated with the indicated concentrations of Fc constructs for 1 h at 37°C. After medium removal, cells were incubated with either enhanced green fluorescent protein (eGFP)-expressing EBOV (Mayinga variant) (55) or with EBOV (Kikwit variant) for 1 h at 37°C (for multiplicity of infection [MOI], see figure legends). Virus was removed, cells were washed three times with phosphate-buffered saline (PBS), and medium was replenished. After 72 h, cells were fixed in 10% neutral-buffered formalin (ValTech Diagnostics) for 72 h. For experiments with eGFP-expressing EBOV, the percentages of eGFP-expressing cells were determined by Discovery-1 automated microscopy (Molecular Devices) measuring nine individual spots per well. In the case of Marburg virus, Vero E6 cells were preincubated with the indicated concentrations of Fc constructs for 1 h at 37°C (for MOIs, see figure legends). After medium removal, cells were incubated with MARV (Ci67 variant) for 1 h at 37°C. Virus was removed, cells were washed three times with PBS, and medium was replenished. After 72 h, culture supernatants were harvested in TRIzol (Invitrogen). Total RNA from untreated cells (mock) or cells infected with MARV was prepared by using a MagMax 96 RNA extraction kit (Ambion). Quantitative reverse transcription-PCR (qRT-PCR) assays were performed using an ABI Prism 7900HT sequence detection system, an RNA UltraSense One-Step kit (Invitrogen), and TaqMan probes (Applied Biosystems) in accordance with the manufacturers' instructions. The final concentrations used in the 20- $\mu$ l reaction mix contained 5  $\mu$ l of RNA, 0.4  $\mu$ M concentrations of each primer (MARV\_GP2\_F, TCACTG AAGGGAACATAGCAGCTAT; MARV\_GP2\_R, TTGCCCGGAGAAAATC ATTT), 0.2  $\mu$ M probe (MARV\_GP2\_P, 6-FAM-ATTGTCAATAAGACAGTG CAC-MGB, where FAM is 6-carboxyfluorescein and MGB is minor groove binder), 4  $\mu$ l of 5 $\times$  reaction mix, 0.4  $\mu$ l of 6-carboxy-X-rhodamine (ROX), and 1  $\mu$ l of enzyme mix (the reaction cycle consisted of reverse transcription at 50°C for 20 min, initial denaturation at 95°C for 2 min, and amplification for 40 cycles at 95°C for 15 s and 60°C for 30 s). Serial 10-fold dilutions of MARV (10<sup>2</sup> to 10<sup>7</sup> copies) were used as standards. Alternatively, cells were fixed in 10% neutral-buffered formalin for 72 h and stained for quantitative image-based analysis with mouse monoclonal antibodies against EBOV GP<sub>1,2</sub> (6D8) or MARV GP<sub>1,2</sub> (9G4), followed by Alexa Fluor 488 goat anti-mouse IgG (Invitrogen). Infected cells were stained with Hoechst 33342 and HCS CellMask Red (Invitrogen). Fluorescent images were acquired on an Opera confocal reader (model 3842, quadruple excitation high sensitivity [QEHS]; Perkin Elmer) using a 10 $\times$  air objective. Analysis of the images was accomplished within the Opera environment using standard Acapella scripts examining  $\approx$ 8,000 cells per sample.

**Construction of  $\Delta$ -peptide-encoding genes, variants, and control proteins.** Codon-optimized open reading frames encoding the Ebola virus, Reston virus, Sudan virus, and Tai Forest virus  $\Delta$ -peptides (GenBank NP\_066247, NP\_690584, AAU43886, and AAB37092, respectively), as well as the EBOV secreted glycoproteins sGP and ssGP (NP\_066247 and NP\_066248, respectively) lacking signal sequences were synthesized by *de novo* recursive PCR. ORFs encoding the  $\Delta$ -peptides of Bundibugyo virus (BDBV) and Reston virus variant BulaA (RESTV-BulaA) were synthesized commercially by DNA 2.0. ORFs were ligated into a pCDM8-derived expression vector (53) encoding the CD5 signal sequence upstream of the ORF insert and the Fc region of human immunoglobulin G1 (Fc) downstream. Plasmids encoding Fc fusion variants of the MARV, EBOV, and SUDV receptor-binding regions (RBRs consisting of MARV residues 38 to 188 fused to Fc and EBOV/SUDV residues 54 to 201 fused to Fc [MARV 38-188-Fc and EBOV/SUDV 54-201-Fc], respectively) and other proteins (human immunodeficiency virus type 1 [HIV-1] gp120-Fc, influenza A virus [FLUAV] HA7 and NA1, Lassa virus [LASV] GPC, lymphocytic choriomeningitis virus [LCMV] GPC, Machupo virus [MACV] GP1 $\Delta$ -Fc and GPC, MARV GP<sub>1,2</sub>-C9, and vesicular stomatitis Indiana virus [VSIV] G) have been described previously (9, 34, 50). Vectors encoding N- and C-terminal truncation variants of  $\Delta$ -peptides, including the Fc-only control, were generated by inverse PCR. Plasmids encoding point mutants were generated using the QuikChange method (Stratagene). Plasmids encoding Reston-Sudan or Sudan-Reston  $\Delta$ -peptide chimeras were synthesized by consecutive PCRs.

**Expression of Fc-tagged  $\Delta$ -peptides, variants, and control proteins.** Proteins were purified as previously described (9). Briefly, HEK 293T cells were transfected with plasmids encoding Fc-fusion  $\Delta$ -peptides, variants, or control proteins using the calcium-phosphate method and grown in 293 SFM II medium (Gibco-Invitrogen). Media were harvested, and proteins were precipitated with protein A-Sepharose Fast Flow beads (GE Healthcare), eluted with 50 mM sodium citrate-50 mM glycine, pH 2, neutralized with sodium hydroxide, dialyzed in PBS, and concentrated. Purified proteins were assayed by SDS-PAGE, followed by Bio-Safe Coomassie staining (Bio-Rad), and quantified by using a Micro BCA (bicinchoninic acid) protein assay kit (Pierce).

**Cell-binding assays.** Cell-binding assays were performed as described previously (9). Fc constructs were added to  $3 \times 10^5$  to  $5 \times 10^5$  cells to a final concentration of 100 to 200 nM and incubated on ice for 1 h. Cells with bound proteins were incubated for 45 min on ice with a 1:40 dilution of goat fluorescein isothiocyanate (FITC)-conjugated anti-human Fc antibody (Sigma-Aldrich) and fixed with PBS–2% formaldehyde. Cell surface binding of constructs was detected by flow cytometry with 10,000 events counted per sample. Baseline fluorescence was determined by measuring cells treated only with goat FITC-conjugated anti-human Fc antibody, which was then subtracted from binding values of the tested constructs and control proteins.

**Transduction assays.** To generate retroviral pseudotypes, HEK 293T cells were transfected by the calcium-phosphate method with plasmid encoding (i) FLUAV HA7 and NA1, LASV GPC, LCMV GPC, MACV GPC, MARV GP<sub>1,2</sub>-C9, or VSIV G, together with (ii) the pQCXIX vector (Clontech) expressing enhanced green fluorescent protein (eGFP) flanked by the Moloney murine leukemia virus (MLV) long terminal repeats, and (iii) plasmid encoding the MLV *gag-pol* genes as described previously (9, 34, 54). Cell supernatants were cleared of cellular debris by centrifugation and filtration and added to permissive cells in the presence of the indicated concentrations of Fc constructs. Volumes of supernatants were adjusted to ensure a transduction rate of  $\approx 30\%$ . After 5 h, cells were replenished with fresh medium. After 36 to 48 h, cells were detached with trypsin (Gibco-Invitrogen) and fixed with PBS–2% formaldehyde. eGFP expression was detected by flow cytometry with 10,000 events counted per sample. Baseline fluorescence was determined by measuring cells exposed to mock control (medium), which was then subtracted from measured values of cells exposed to pseudotypes. Samples containing pseudotypes only (absence of Fc constructs) were taken as positive controls and normalized to 100% transduction.

## RESULTS

**Ebola virus  $\Delta$ -peptide-Fc, but not sGP-Fc or ssGP-Fc, binds to filovirus-permissive cells and inhibits marburgvirus and ebolavirus GP<sub>1,2</sub>-mediated cell entry.** Fc-tagged Ebola virus (EBOV) and Marburg virus (MARV) GP<sub>1</sub>, and especially the receptor-binding regions therein (RBR-Fcs), bind specifically to filovirus-permissive, but not to filovirus-resistant, cells, and both inhibit cell entry of MARV and EBOV (21). We assumed that Fc-tagged EBOV sGP and ssGP, both of which contain the EBOV GP<sub>1</sub> RBR but differ from GP<sub>1</sub> in their C termini, behave similarly to both RBR-Fcs. To test this hypothesis, we purified EBOV sGP-Fc, ssGP-Fc, and an assumed negative control,  $\Delta$ -peptide-Fc ( $\Delta$ -Fc), from HEK 293T cells (Fig. 1A). Equivalent concentrations of each protein were incubated with filovirus-permissive Vero E6 (5, 10, 43, 47) (Fig. 1B) or HeLa cells (5) (Fig. 1C) or with filovirus-resistant Jurkat E6-1 lymphocytes (5) (Fig. 1D). Cell surface association of each protein was determined by flow cytometry using a FITC-conjugated anti-Fc secondary antibody. Fc alone, Fc-tagged severe acute respiratory syndrome coronavirus receptor-binding domain (SARS-CoV RBD-Fc), HIV-1 gp120 (HIV-1 gp120-Fc) (59), MACV receptor-binding domain (MACV GP1 $\Delta$ -Fc) (35), and EBOV RBR (EBOV 54-201-Fc) (21) were used as controls. All controls behaved as expected. Fc did not bind to any cell type tested. SARS-CoV RBD-Fc bound to Vero E6 cells, which naturally express the SARS-CoV receptor, angiotensin-converting enzyme 2, but not to HeLa cells or Jurkat E6-1 lymphocytes, which do not (25). HIV-1 gp120-Fc bound Jurkat E6-1 lymphocytes, which naturally express the principle HIV-1 receptor, CD4, but not to Vero E6 or HeLa cells, which do not (7, 18). MACV GP1 $\Delta$ -Fc bound to Vero E6, HeLa, and Jurkat E6-1 cells, which express the MACV receptor, transferrin receptor 1 (35). To our surprise, little to no association with Vero E6 or HeLa cells was measured with EBOV sGP-Fc and ssGP-Fc, whereas EBOV  $\Delta$ -Fc bound these cells even more efficiently than EBOV 54-201-Fc. On the other hand, none of the

three secreted EBOV glycoproteins (sGP-Fc, ssGP-Fc, and  $\Delta$ -Fc) associated with filovirus-resistant Jurkat E6-1 lymphocytes.

We then evaluated whether EBOV sGP-Fc, ssGP-Fc, or  $\Delta$ -peptide-Fc behaves like the EBOV RBR-Fc and inhibits Marburg virus GP<sub>1,2</sub>-mediated cell entry, possibly by binding to the shared filovirus receptor (21, 29). A Moloney murine leukemia virus vector expressing eGFP was pseudotyped with the spike protein GP<sub>1,2</sub> of Marburg virus (MARV/MLV). MARV GP<sub>1,2</sub> was chosen for this experiment because both Marburg virus and Ebola virus RBRs (MARV 38-188-Fc and EBOV 54-201-Fc, respectively) inhibit either EBOV/MLV or MARV/MLV and because MARV/MLV was easier to produce in large quantities and was more stable than EBOV/MLV when stored over longer periods of time (21). Vero E6 cells were incubated with EBOV sGP-Fc, ssGP-Fc,  $\Delta$ -Fc or control proteins and MARV/MLV (Fig. 1E). As expected, control proteins SARS-CoV RBD-Fc and Fc had little and no effect on transduction efficiency, respectively. In accordance with the cell-binding data, EBOV sGP-Fc and ssGP-Fc inhibited cell transduction by MARV/MLV only minimally, whereas EBOV  $\Delta$ -Fc inhibited MARV/MLV transduction approximately 2-fold more efficiently than the EBOV 54-201-Fc positive control. These data surprisingly indicate that Fc-tagged EBOV  $\Delta$ -peptide, for which there is no equivalent in the MARV proteome, can interfere with MARV GP<sub>1,2</sub>-mediated entry.

**Fc-tagged Ebola virus, Sudan virus, and Taï Forest virus, but not Reston virus and Bundibugyo,  $\Delta$ -peptides inhibit filovirus GP<sub>1,2</sub>-mediated cell entry and infection of Marburg and Ebola virus in a dose-dependent manner.** We purified  $\Delta$ -Fc of three other ebolaviruses, RESTV, SUDV, and TAFV, from HEK 293T cells (Fig. 2A). Equivalent concentrations of each  $\Delta$ -Fc were incubated with filovirus-permissive Vero E6 cells (Fig. 2B), HeLa cells (Fig. 2C), or filovirus-resistant Jurkat E6-1 lymphocytes (Fig. 2D), and cell surface association of each protein was determined by flow cytometry. Fc, SARS-CoV RBD-Fc, HIV-1 gp120-Fc, MACV GP1 $\Delta$ -Fc, and EBOV 54-201-Fc were used as controls. All Fc-tagged ebolavirus  $\Delta$ -peptides associated with the cell surface of Vero E6 and HeLa cells. EBOV  $\Delta$ -Fc bound to the surface of these cells with much higher affinity than SUDV and TAFV  $\Delta$ -Fc, whereas RESTV  $\Delta$ -Fc exhibited the least efficient binding phenotype. In contrast, none of the Fc-tagged ebolavirus  $\Delta$ -peptides bound to Jurkat E6-1 lymphocytes.

The ability of the four ebolavirus  $\Delta$ -Fc to inhibit entry of pseudotyped gammaretrovirus particles was again assayed using MARV/MLV (Fig. 2E). Fc, SARS-CoV RBD-Fc, and MARV 38-188-Fc (21) were used as controls. EBOV, SUDV, and TAFV  $\Delta$ -Fc efficiently inhibited cell transduction by MARV/MLV in a dose-dependent manner and at low molarity. Surprisingly, SUDV  $\Delta$ -Fc and TAFV  $\Delta$ -Fc were more efficient inhibitors than EBOV  $\Delta$ -Fc and MARV 38-188-Fc (50% inhibitory concentration [IC<sub>50</sub>] of  $\approx 25$  nM in this assay for SUDV and TAFV  $\Delta$ -Fc). In accordance with the cell-binding data, RESTV  $\Delta$ -Fc inhibited transduction much less efficiently than the other  $\Delta$ -peptides. EBOV  $\Delta$ -Fc was a relatively weak inhibitor despite its consistently strong cell surface binding, an observation which at this time we can only speculate to be due to unspecific cell surface binding via its extensive O-glycosylation (54).

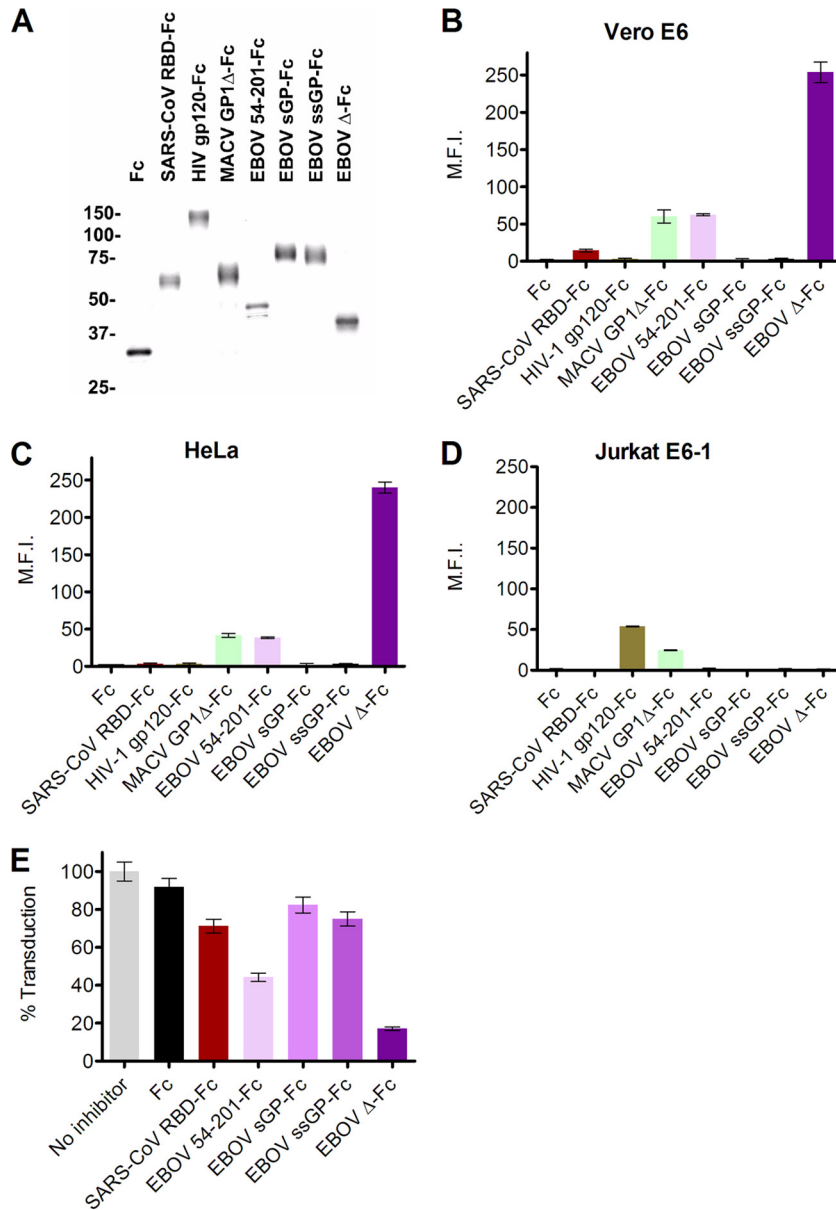


FIG. 1. Expression, cell surface binding, and cell entry-inhibitory effect of EBOV sGP-Fc, ssGP-Fc, and Δ-peptide-Fc. (A) EBOV sGP-Fc, ssGP-Fc, Δ-Fc, and control proteins Fc, SARS-CoV RBD-Fc, HIV-1 gp120-Fc, MACV GP1Δ-Fc, and EBOV 54-201-Fc were purified from transfected cells and visualized by Coomassie staining. (B, C, and D) Proteins (100 nM) were incubated with filovirus-permissive Vero E6 or HeLa cells or filovirus-resistant Jurkat E6-1 lymphocytes and analyzed by flow cytometry. MFI, mean fluorescence intensity. (E) EBOV sGP-Fc, ssGP-Fc, or Δ-Fc or control proteins (200 nM) were incubated with Vero E6 cells and eGFP-expressing MLV particles pseudotyped with MARV GP<sub>1,2</sub>. Entry of pseudotyped MLV was quantified by measuring green fluorescence. Error bars indicate standard deviations.

To determine whether Fc-tagged ebolavirus Δ-peptides also inhibit infectious filoviruses, Vero E6 cells were preincubated with EBOV, RESTV, SUDV, and TAFV Δ-Fcs or SARS-CoV RBD-Fc and exposed to infectious EBOV-eGFP (Fig. 3A). In accordance with the results obtained with pseudotyped MLV particles (Fig. 2E), virus infection, measured as the percentage of infected cells, was specifically inhibited by EBOV, SUDV, and TAFV Δ-Fcs. SUDV and TAFV Δ-Fcs were again the most efficient inhibitor, whereas RESTV Δ-Fc did not inhibit EBOV-eGFP infection and behaved like the SARS-CoV RBD-Fc negative control. To confirm the data obtained

with MARV/MLV, we next tested the effect of Fc-tagged Δ-peptides on MARV infection. For this assay, we used a 10-fold higher MOI (MOI of 10) than in the EBOV-eGFP experiment (MOI of 1) to determine whether inhibitory effects of Δ-peptides remain visible under high virus concentrations. In addition to Fc-tagged EBOV, SUDV, and RESTV Δ-peptides, we also tested the Fc-tagged Δ-peptides of the recently discovered Bundibugyo virus and of a RESTV recently isolated from domestic pigs in the Philippines (RESTV-BulaA) (Fig. 3B). In accordance with the results obtained with MARV/MLV and infectious EBOV-eGFP, we found that EBOV and

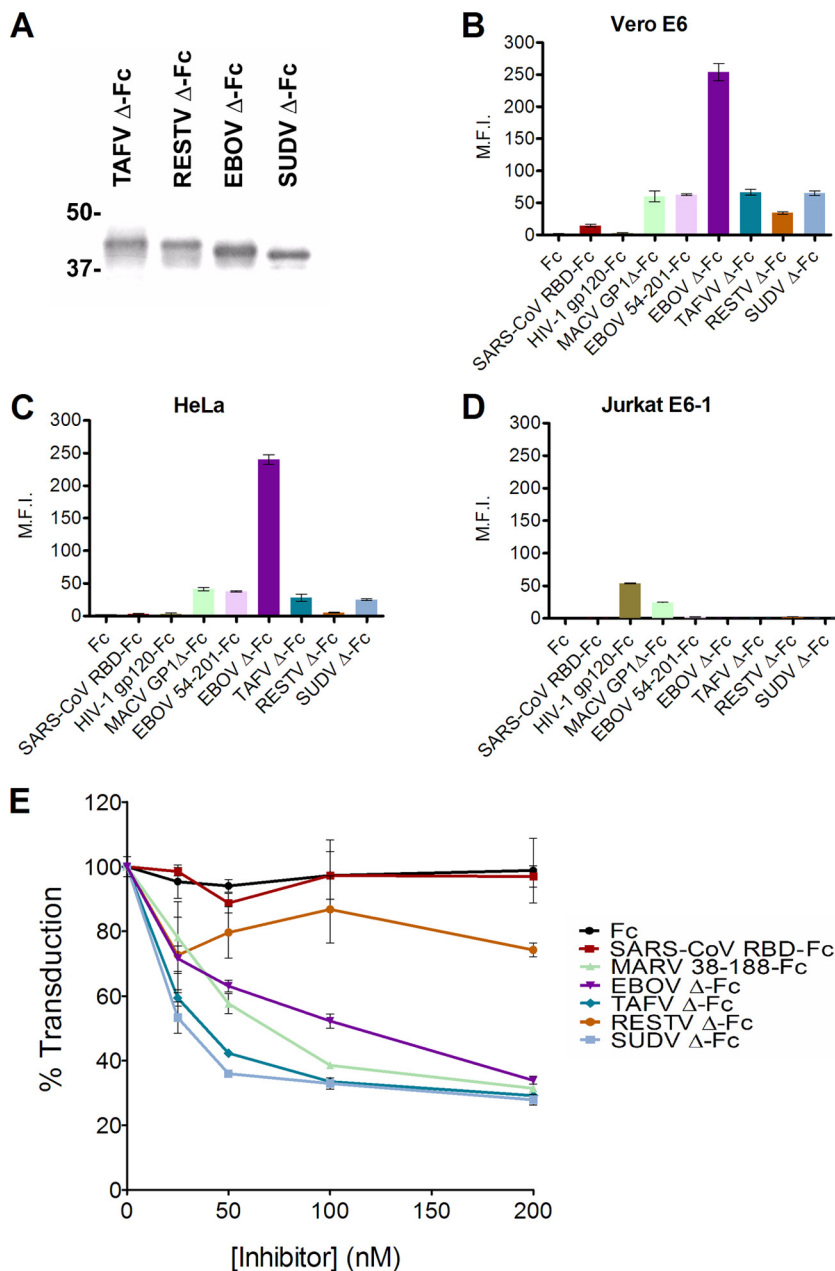


FIG. 2. Expression, cell surface binding, and cell entry-inhibitory effect of TAFV, SUDV, RESTV, and EBOV Δ-peptide-Fcs. (A) EBOV, RESTV, SUDV, and TAFV Δ-Fc were purified from transfected cells and visualized by Coomassie staining. (B, C, and D) Δ-Peptide-Fcs or control proteins (100 nM) were incubated with Vero E6 or HeLa cells or with Jurkat E6-1 lymphocytes and analyzed by flow cytometry. (E) The indicated concentrations of Δ-Fcs or control proteins Fc, SARS-CoV RBD-Fc, or MARV 38-188-Fc were incubated with Vero E6 cells and eGFP-expressing MLV pseudotyped with MARV GP<sub>1,2</sub>. Entry of pseudotyped MLV was quantified by measuring green fluorescence. Error bars indicate standard deviations.

SUDV Δ-Fcs inhibited MARV infection, whereas RESTV Δ-Fc had little effect. Additionally, we found BDBV Δ-Fc to have no phenotype in this assay, whereas RESTV-BulaA Δ-Fc was an efficient inhibitor. These data demonstrate that EBOV, SUDV, and TAFV Δ-peptides, in addition to their inhibitory effect on MARV GP<sub>1,2</sub>-mediated entry, also inhibit infectious EBOV and/or MARV infection. This supports the notion that Δ-peptides interact with a factor engaged by both marburgviruses and ebolaviruses to gain entry into target cells.

**Fc-tagged ebolavirus Δ-peptides specifically inhibit marburgvirus and ebolavirus GP<sub>1,2</sub>-mediated entry.** We continued our experiments with SUDV Δ-Fc as we had determined this construct to be a very efficient EBOV and MARV infection inhibitor, with the additional advantage of expressing to much higher levels than the almost equally efficient TAFV Δ-Fc. To evaluate whether ebolavirus Δ-peptide Fc fusion proteins specifically inhibit filovirus cell entry, Vero E6 cells were incubated with SUDV Δ-Fc or SARS-CoV RBD-Fc control and

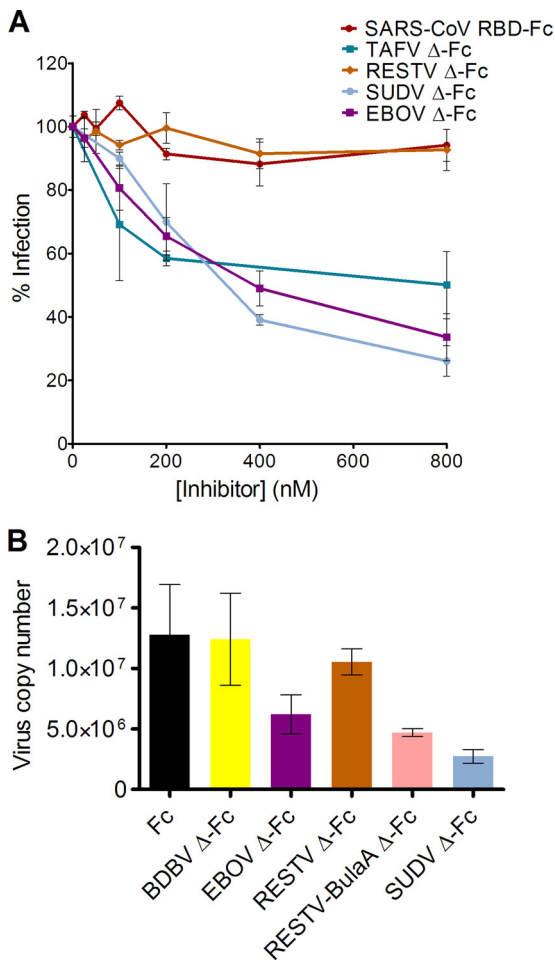


FIG. 3. EBOV, SUDV, and TAFV, but not RESTV, Δ-peptide-Fcs inhibit filoviruses infection. (A) Vero E6 cells incubated with Fc constructs were infected with EBOV-eGFP (MOI of 1). Infection was quantified by measuring green fluorescence. Error bars indicate standard deviations. (B) Vero E6 cells incubated with Fc constructs were infected with MARV (MOI of 10). Infection was quantified by qRT-PCR. Error bars indicate standard deviations.

MLV pseudotyped with the surface proteins of human influenza A virus (FLUAV/MLV), Lassa virus (LASV/MLV), Machupo virus (MACV/MLV), vesicular stomatitis Indiana virus (VSIV/MLV), lymphocytic choriomeningitis virus (LCMV/MLV) or Marburg virus (MARV/MLV) (Fig. 4). As expected, SARS-CoV RBD-Fc had no effect on cell transduction by either MLV, and SUDV Δ-Fc did not inhibit cell transduction by MLV pseudotyped with nonfilovirus spike proteins. However, SUDV Δ-Fc again inhibited MARV/MLV transduction, indicating that ebolavirus Δ-peptides specifically modulate filovirus cell entry.

**Mutational analysis of Fc-tagged Sudan virus Δ-peptide.** Next, we wanted to determine the functional region of SUDV Δ-Fc. Individual SUDV Δ-peptide residues were mutated to alanine, and N- and C-terminal truncations of SUDV Δ-peptide were created to evaluate which parts of the peptide are crucial for its function. Chimeras of SUDV and RESTV Δ-peptides were synthesized to understand why RESTV Δ-Fc is the only tested ebolavirus Δ-peptide that did not inhibit

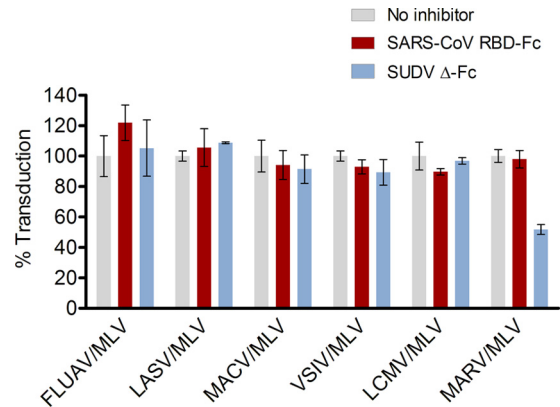


FIG. 4. SUDV Δ-peptide-Fc specifically inhibits filovirus GP<sub>1,2</sub>-mediated entry. SUDV Δ-Fcs (100 nM) were incubated with Vero E6 cells together with eGFP-expressing MLV pseudotyped with the spike proteins of either FLUAV, LASV, MACV, VSIV, LCMV, or MARV. MLV entry was quantified by measuring green fluorescence. Error bars indicate standard deviations.

EBOV and MARV infection (Fig. 5A). Three N-terminal truncation mutants of SUDV (SUDV Δ7-48-Fc, SUDV Δ13-48-Fc, and SUDV Δ18-48-Fc) could not be expressed. All other constructs were purified from HEK 293T cells (Fig. 5B). Equivalent concentrations of these proteins were incubated with Vero E6 cells (Fig. 5C) or with Jurkat E6-1 lymphocytes (Fig. 5D), and cell surface association of each protein was determined as described above. Fc, SARS-CoV RBD-Fc, and HIV-1 gp120-Fc were used as controls. A C-terminal truncation variant of SUDV lacking residues 1 to 39 (SUDV Δ1-39-Fc) bound as efficiently to Vero E6 cells as wild-type SUDV Δ-Fc, while a further C-terminal truncation reduced (SUDV Δ1-33-Fc) or abolished (SUDV Δ1-28-Fc) cell surface association. An SUDV mutant with the mutation of T9 to A (ΔT9A-Fc) was created to evaluate whether a computationally predicted O-glycosylation site within SUDV Δ-peptide plays an important role in Fc-tagged Δ-peptide-mediated filovirus cell entry inhibition. ΔT9A-Fc bound to Vero E6 cells with increased affinity compared to Δ-Fc, and Δ1-39-Fc with the T9A mutation (Δ1-39T9A-Fc) bound cells comparably to Δ1-39-Fc. The exchange of Δ-Fc residue R21 for alanine did not have an effect on cell association, whereas simultaneous exchange of C29 and C38, which are absolutely conserved among all ebolavirus Δ-peptides, for alanine residues surprisingly increased cell binding. None of the created Δ-peptide mutants bound to filovirus-resistant Jurkat E6-1 lymphocytes.

The ability of mutated SUDV Δ-Fcs to inhibit entry of pseudotyped retrovirus particles was assayed as described above, using MARV/MLV (Fig. 5E). SRΔ-Fc, a chimeric Δ-peptide consisting of the N-terminal half of SUDV Δ-peptide and the C-terminal half of RESTV Δ-peptide, inhibited cell transduction only minimally and at levels comparable to RESTV Δ-Fc. Conversely, RSΔ-Fc, a chimeric Δ-peptide consisting of the N-terminal half of RESTV Δ-peptide and the C-terminal half of SUDV Δ-peptide, strongly inhibited transduction at levels comparable to SUDV Δ-Fc. Successive C-terminal truncation of SUDV Δ-Fc decreased cell-surface binding (Fig. 5C), as well as transduction inhibition (Δ1-39-Fc > Δ1-33-Fc > Δ1-28-Fc > 1-17-Fc). The N-terminal truncation variant Δ28-48-Fc, which

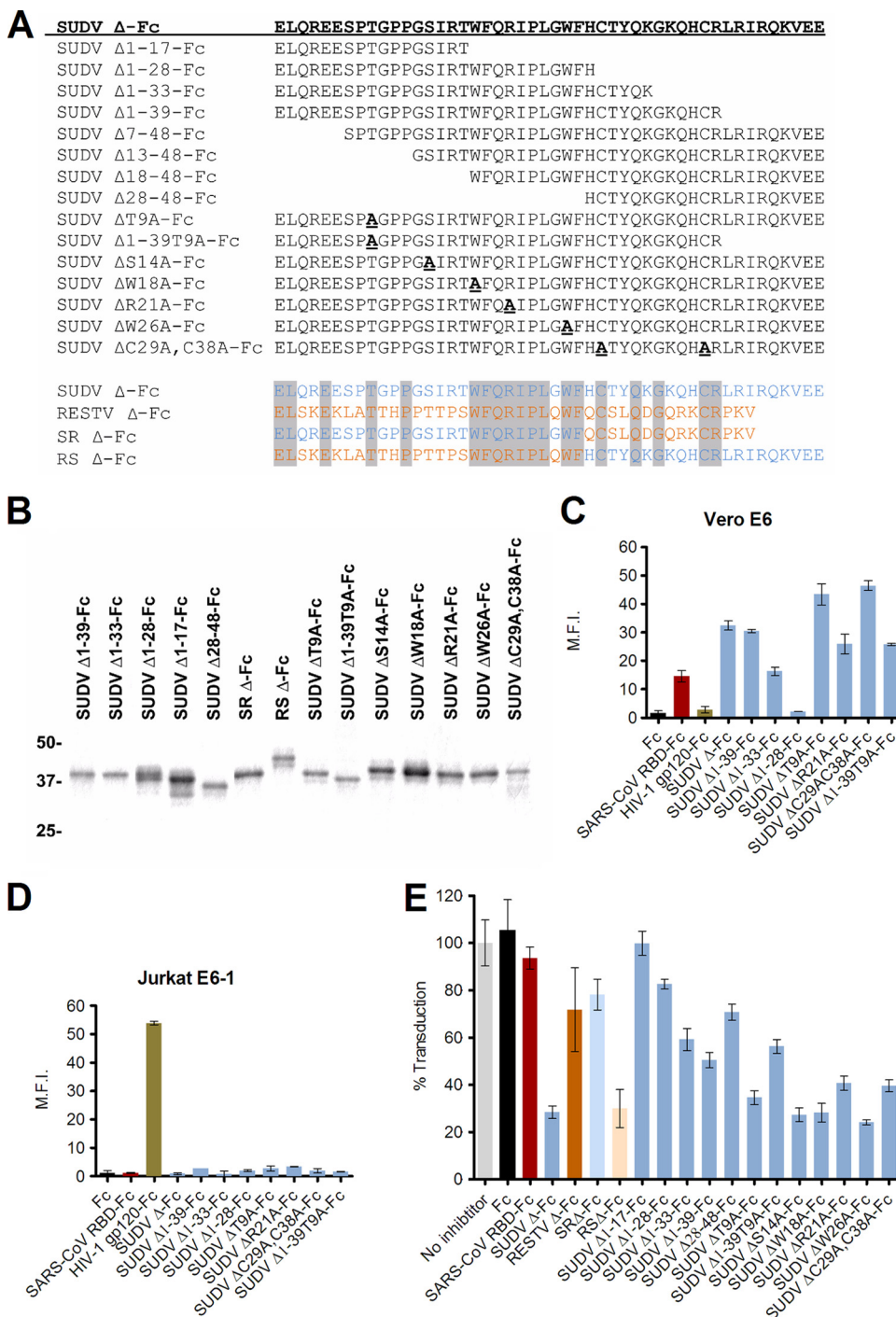


FIG. 5. Effect of SUDV Δ-peptide-Fc mutants on filovirus GP<sub>1,2</sub>-mediated entry. (A) Overview of SUDV Δ-peptide-Fc mutants. In the top panel, introduced alanine residues are bold and underlined. The Sudan-Reston Δ-Fc chimera (SRΔ-Fc) and Reston-Sudan Δ-Fc chimera (RSΔ-Fc) are shown in the lower panel. Residues unique to SUDV, unique to RESTV, or shared among them are highlighted in light gray, not highlighted, or highlighted in dark gray, respectively. (B) SUDV Δ-Fc mutants were purified from transfected cells and visualized by Coomassie staining. (C and D) SUDV Δ-Fc mutants or control proteins Fc, SARS-CoV RBD-Fc, HIV-1 gp120-Fc, or wild-type SUDV Δ-Fc (100 nM) were incubated with Vero E6 cells or Jurkat E6-1 lymphocytes and analyzed by flow cytometry. (E) SUDV Δ-Fc mutants or control proteins (100 nM) were incubated with Vero E6 cells and eGFP-expressing MLV pseudotyped with MARV GP<sub>1,2</sub>. MLV entry was quantified by measuring green fluorescence. Error bars indicate standard deviations.

represents the C-terminal half of SUDV Δ-Fc, barely inhibited cell transduction. SUDV ΔT9A-Fc, ΔS14A-Fc, ΔW18A-Fc, and ΔW26A-Fc were not impaired in their ability to inhibit pseudotype entry compared to wild-type SUDV Δ-Fc, whereas

ΔR21A-Fc and the double mutant ΔC29A C38A-Fc inhibited entry less efficiently. These data indicate that SUDV Δ-Fc exerts its entry-inhibitory effect primarily through amino acid residues located in its C terminus.

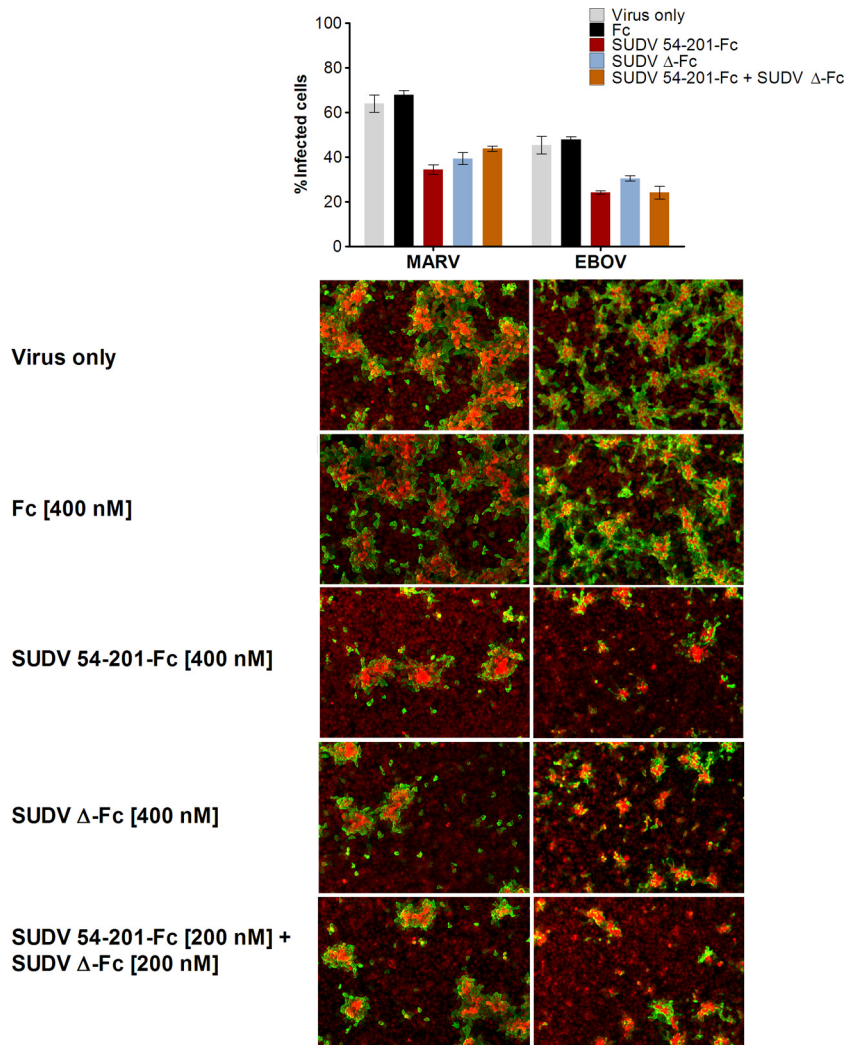


FIG. 6. SUDV Δ-Fc and RBR-Fc do not function synergistically. (Top) Vero E6 cells incubated with Fc constructs (total of 400 nM) were infected with MARV (left panel) or EBOV (right panel) at an MOI of 3. Infection was quantified by high-content image-based analysis of filovirus-infected cells stained with monoclonal antibodies targeting MARV or EBOV GP<sub>1,2</sub>. Error bars indicate standard deviations. (Bottom) Representative images of the results presented in the top panel are shown. Filovirus-infected cells are shown in green and cytoplasmic/nuclear staining is shown in red.

**Fc-tagged Sudan virus receptor-binding region and Sudan virus Δ-peptide do not act synergistically.** It is possible that the receptor-binding region of filovirus GP<sub>1</sub> and ebolavirus Δ-peptides exert their actions at different steps during the filovirus life cycle. If so, both could either act additively or synergistically. To test this hypothesis, we incubated Vero E6 cells with 400 nM Fc control, 400 nM SUDV receptor-binding region (54-201-Fc), 400 nM SUDV Δ-Fc, or a combination of 200 nM SUDV 54-201-Fc together with 200 nM SUDV Δ-Fc and then infected the cells with either MARV or EBOV as described above. Analysis of the infection rates, using specific monoclonal antibodies against MARV and EBOV GP<sub>1,2</sub> and an Alexa Fluor 488 anti-Fc antibody, revealed that the combination of 200 nM RBR-Fc and 200 nM Δ-Fc inhibited virus infection to levels similar to those of 400 nM RBR-Fc or 400 nM Δ-Fc alone (Fig. 6). We therefore conclude that both virus infection

inhibitors do not act synergistically when present at the same time.

### DISCUSSION

We are currently addressing two hypotheses as to the role of Δ-peptides in pathogenesis. First, the peptides could prevent superinfection of producer cells by binding to a cell surface filovirus receptor. Low-level expression of EBOV spike protein enhances, but high-level expression inhibits, cell transduction with MLV/EBOV, and low-level expression did not have an effect on MLV/MARV cell entry, whereas high-level expression inhibited it (28). These data imply that ebolavirus-infected cells may be prone to superinfection early in infection and that Δ-peptide could counter this susceptibility. Δ-peptides also could interfere with steps of the virus entry process other than



cell surface factor binding, such as glycoprotein processing by cathepsins or the yet still hypothetical protease-requiring factor that acts after cathepsin cleavage (6, 41). Preliminary experiments suggest, however, that the peptides do not affect the activity of cathepsin B in *in vitro* enzymatic assays (data not shown). Second, it is possible that  $\Delta$ -peptides prevent the association of maturing ebolavirus GP<sub>1,2</sub> with a receptor or a coreceptor during synthesis in the ER of an infected cell and thereby prevent trapping of budding progeny virions. Both strategies are, indeed, being used by other viruses. For instance, HIV-1 Nef downregulates the expression of the HIV-1 receptor CD4 to prevent superinfection (1) and circumvents premature fusion by inhibiting the engagement of CD4 with the spike protein gp160 in the Golgi network (27). Overexpression of CD4 in HIV-1-infected cells, on the other hand, reduces infectivity via the sequestering of gp160 by CD4 (22). Furthermore, HIV-1 Vpu mediates endoplasmic reticulum (ER)-associated protein degradation (ERAD) of CD4 to prevent the formation of CD4-gp160 complexes (58). In the case of influenza viruses, neuraminidase (NA) limits superinfection of the producer cell by cleaving sialic acids, the receptors of these viruses (15), an activity that is also necessary for the release of progeny viruses (55). Marburgviruses, which do not express  $\Delta$ -peptides, may have developed an alternative way to prevent superinfection and/or tethering to the plasma membrane.

The EBOV RBR is present in GP<sub>1</sub> (residues 54 to 201), sGP, and ssGP. We therefore hypothesized that EBOV sGP-Fc and ssGP-Fc bind to the surface of filovirus-permissive cells, but not filovirus-resistant cells, and inhibit filovirus entry, thus mimicking previously described properties of GP<sub>1</sub>-Fc and its mutants (21). Unexpectedly, we discovered that the C-terminal cleavage product that is produced during sGP maturation,  $\Delta$ -peptide, fulfilled these expectations when fused to Fc, whereas sGP-Fc and ssGP-Fc did not (Fig. 1). The latter observation can be explained if one assumes that the unique C termini of sGP and ssGP influence their tertiary and quaternary structures and thus their ability to modulate entry. Indeed, antibodies from survivors of EBOV infection preferentially react with either GP<sub>1,2</sub> or sGP (31, 32). Moreover, GP<sub>1,2</sub> assumes a trimeric conformation (23), whereas sGP assembles as a parallel homodimer using two intermolecular disulfide bonds at the N and C termini of each monomer (3). ssGP is secreted as a homodimer that is held together by a single intermolecular disulfide bond (33). The oligomeric state of  $\Delta$ -peptides remains to be determined. Initial experiments evaluating SUDV  $\Delta$ -peptide tagged N-terminally with a FLAG tag instead of a C-terminal Fc tag demonstrate that this most likely monomeric variant does not inhibit Marburg virus infection (Fig. 7). The two conserved cysteine residues in ebolavirus  $\Delta$ -peptides (Fig. 8 gives sequence information) and the homodimerization of the  $\Delta$ -peptide precursor, pre-sGP (3, 11, 53), suggest that  $\Delta$ -peptides are most likely dimers. If that indeed is the case, it is plausible that the inhibitory effect of  $\Delta$ -peptide is dependent on its dimeric state, and therefore only an Fc  $\Delta$ -peptide fusion (dimeric due to the Fc tag) acts as an effective inhibitor. We have thus far failed in raising useful antibodies against  $\Delta$ -peptides using commercial services and also in procuring sufficient amounts of sera of nonhuman primates that were infected with filoviruses but survived long

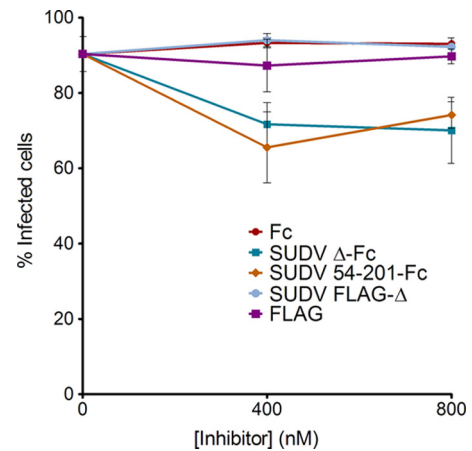


FIG. 7. Evaluation of FLAG-tagged Sudan  $\Delta$ -peptide as an inhibitor of MARV infection. Fc constructs, N-terminally FLAG-tagged SUDV  $\Delta$ -peptide, or FLAG tag alone was incubated with Vero E6 cells at the indicated concentrations. Cells were then infected with MARV (MOI of 5), and infection rates were measured as described in the legend of Fig. 6.

enough to mount an antibody response. Therefore, it remains to be seen in which quantity and which tissues  $\Delta$ -peptides are produced in a filovirus-infected animal.

The observed effects of Fc-tagged ebolavirus  $\Delta$ -peptides are most intriguing since thus far they were regarded as nonfunctional by-products of sGP maturation (54) and because the peptides' primary sequences are not similar to the filovirus RBRs or to any other known protein. SUDV and TAFV  $\Delta$ -Fc inhibited infectious EBOV and MARV infection more efficiently than EBOV  $\Delta$ -Fc (Fig. 3), suggesting that they could be developed as novel antivirals. Consequently, we have begun to evaluate their efficacy in rodent models of filovirus disease.

Interestingly,  $\Delta$ -Fc of RESTV, the only ebolavirus nonpathogenic for humans (2, 34), did not inhibit EBOV or MARV infection (Fig. 3). Since RESTV is as virulent for nonhuman primates, such as cynomolgus macaques, as EBOV and MARV, this observation leads to the fascinating hypothesis that  $\Delta$ -peptides could play important roles in filovirus pathogenesis in different hosts or in filovirus persistence in their reservoirs—now thought to be frugivorous bats (24, 45). Indeed, recently performed experiments demonstrated that a recombinant guinea pig-adapted EBOV tailored not to produce sGP/ $\Delta$ -peptide is severely attenuated in guinea pigs compared to parent guinea pig-adapted virus. Furthermore, passaging of wild-type Ebola virus in Vero E6 cells led to the evolution of variants with a modified GP gene editing site ("8U virus"), which produces predominantly GP<sub>1,2</sub> and little sGP/ $\Delta$ -peptide, whereas infection of guinea pigs with 8U virus rapidly resulted in the evolution of "7U viruses," thereby "correcting" the ratio of GP<sub>1,2</sub> to sGP/ $\Delta$ -peptide to large amounts of the latter. These data suggest that the wild-type 7U virus has a selective advantage in animals for yet unknown reasons and that the production of larger amounts of sGP and thereby  $\Delta$ -peptide are important factors in infection (52).

Computational analyses revealed that the sequences of  $\Delta$ -peptides are highly conserved among the variants of each individual ebolavirus (Fig. 8). For instance, the  $\Delta$ -peptide se-

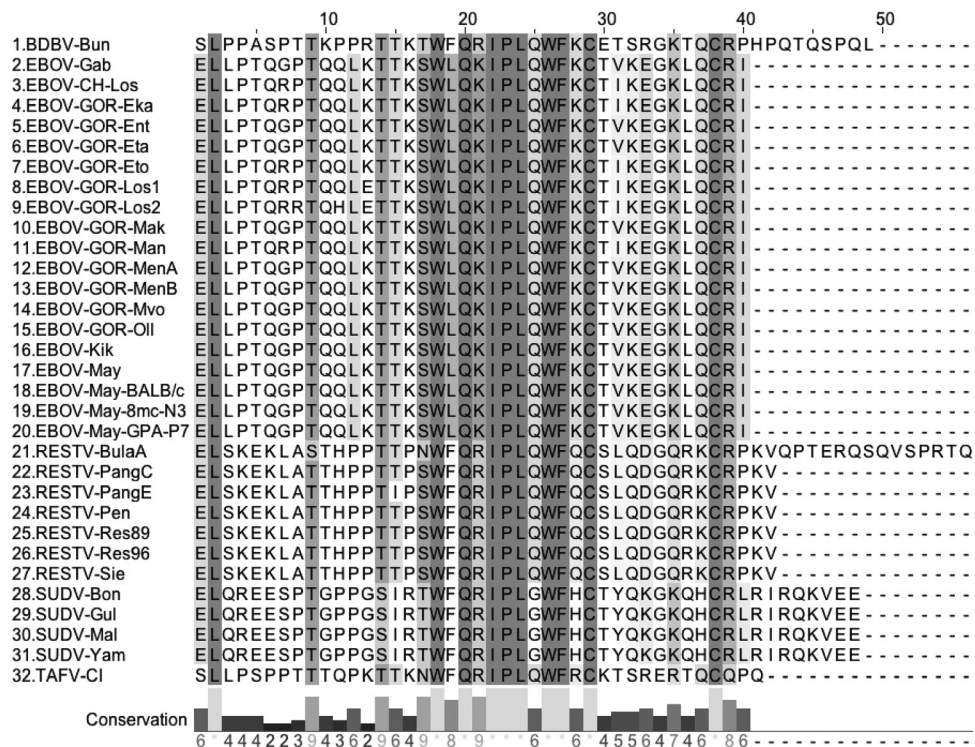


FIG. 8. Sequence alignment of ebolavirus Δ-peptides. Highlighted residues are shaded according to the BLOSUM62 score, which takes into account physico-chemical properties and amino acid characteristics, such as charge or hydrophobicity (4). Conservation is measured as a numerical index reflecting these characteristics in the alignment: identities score highest, followed by the next most conserved group containing substitutions to amino acids assigned to the same physico-chemical class (26). GenBank accession numbers are as follows: 1, FJ217161; 2, EVU77384; 3, EU051633; 4, EU051632; 5, AY526102; 6, AY526100; 7, EU051634; 8, EU051630; 9, EU051631; 10, AY526101; 11, EU051635; 12, AY526105; 13, AY526098; 14, AY526104; 15, AY526099; 16, AY354458; 17, AF086833; 18, AF499101; 19, AF272001; 20, EU224440; 21, FJ621583; 22, FJ621584; 23, FJ621585; 24, AF522874; 25, NC\_004161; 26, AB050936; 27, EVU23417; 28, Q9QP77; 29, AY729654; 30, EVU23069; 31, EU338380; 32, FJ217162. EBOV-May, EBOV Mayinga variant; EBOV-Kik, EBOV Kikwit variant.

quences of all known SUDV strains, isolated over 3 decades from humans, are 100% identical. This extent of conservation is also true for human EBOV variants and mouse- and guinea pig-adapted viruses (EBOV-May BALB/c and -8mc-N3/-GPA-P7, respectively), whereas western lowland gorilla isolates (EBOV-GOR) and central chimpanzee isolates (EBOV-CH) show slight variability. RESTV Δ-peptides of viruses isolated from cynomolgus macaques in 1989, 1992, and 1996 are 100% conserved as well. On the other hand, Δ-peptides of the individual ebolaviruses (the recently described BDBV [46] and EBOV, RESTV, SUDV, and TAFV) vary greatly among each other but share common elements, suggesting that the function of these peptides is important and is conserved across different ebolavirus hosts (Fig. 8).

Recently, RESTV was isolated from domestic pigs from Bulacan (BulaA) and Pangasinan (PangA and PangE) in the Philippines (2). Surprisingly, the PangA and PangE Δ-Fcs of these isolates differ slightly, and the BulaA Δ-Fc differs drastically, from the other known RESTV Δ-peptides (Fig. 8). The BulaA isolate is additionally characterized by a deleterious mutation in the sGP/Δ-peptide furin cleavage site (RARR → RAQR), suggesting that this most divergent RESTV Δ-peptide might not be produced during infection. Interestingly, one of our experiments suggests that RESTV-BulaA Δ-Fc inhibits at least MARV infection (Fig. 3B). This raises the fascinating

hypothesis that Reston viruses have evolved not to produce functional Δ-peptides, either by scrambling their sequence (macaque-derived RESTV) or by preventing their secretion (RESTV-BulaA). Unfortunately, we did not have access to sufficient amounts of high-quality stocks of either macaque- or pig-derived RESTV and could therefore not yet evaluate the effect of RESTV and other filovirus Δ-peptides on RESTV infection. Likewise, one experiment (Fig. 3B) indicates that BDBV Δ-Fc may also be either nonfunctional or specific for BDBV as it had no influence on MARV infection. The function of this particular Δ-peptide will be evaluated in greater detail once we gain access to BDBV and TAFV stocks.

Surprisingly, the conserved sequence in the center of the peptides does not seem to be crucial for their function, as the mutation of several of its residues in SUDV Δ-Fc to alanines (ΔW18A-Fc, ΔR21A-Fc, and ΔW26A-Fc) did not impair cell binding or transduction inhibition considerably (Fig. 5C and E). Similarly, introduction of mutations into the N-terminal half of the peptide (ΔT9A-Fc and ΔS14A-Fc) did not decrease the inhibitory effect on GP<sub>1,2</sub>-mediated cell entry. In contrast, consecutive truncation of the C terminus of SUDV Δ-Fc(Δ1-39-Fc, Δ1-33-Fc, Δ1-28-Fc, and Δ1-17-Fc) did result in progressive loss of function. In addition, a chimera consisting of the N-terminal half of SUDV Δ-peptide and the C-terminal half of RESTV Δ-peptide (SRA-Fc) behaved like full-length

RESTV  $\Delta$ -Fc and inhibited GP<sub>1,2</sub>-mediated cell entry only minimally, whereas a chimera consisting of the N-terminal half of RESTV  $\Delta$ -peptide and the C-terminal half of SUDV  $\Delta$ -peptide (RSD- $\Delta$ -Fc) mimicked SUDV  $\Delta$ -Fc and inhibited transduction efficiently. The  $\Delta$ 28-48-Fc mutant, which consists only of SUDV  $\Delta$ -peptide's C terminus, barely inhibited GP<sub>1,2</sub>-mediated cell entry. These results indicate the following: (i) SUDV  $\Delta$ -peptide possibly requires its N terminus to ensure correct folding, although the N terminus is not involved in attaching to SUDV  $\Delta$ -peptide's cell-surface binding partner; (ii) the inhibitory function of SUDV  $\Delta$ -Fc may be mediated by its C terminus; (iii) T9 of SUDV  $\Delta$ -Fc, which is probably *O*-glycosylated, is not important for function; and (iv) residues S14, R21, W18, and W26 (all located within the N-terminal half of the peptide) and C29/C38 (in the C-terminal half) may not play crucial roles in entry inhibition. A closer look at the C termini of ebolavirus  $\Delta$ -peptides led us to the conclusion that they might exert their inhibitory effects through charged interactions rather than a common structure as no sequence similarity is obvious (Fig. 8). This is not unusual as structural disorder is a hallmark of proteins associated with signaling or regulation (9, 44) and is found among numerous virus proteins that are encoded by overlapping ORFs, allowing them to adopt rapidly interconverting structural shapes (36). Clearly, this hypothesis will have to be tested through the creation of additional mutants.

The observations that several Fc-tagged ebolavirus  $\Delta$ -peptides bind with high efficiency to filovirus-permissive cells but not to filovirus-resistant cells and even more so that they inhibit MARV spike protein-mediated cell entry as well as EBOV and MARV infection clearly suggest that these peptides interfere with a molecule that is engaged during cell entry by both ebolaviruses and marburgviruses.

#### ACKNOWLEDGMENTS

J.H.K. and V.W.-J. performed part of this work as employees of Tunnell Consulting, Inc., a subcontractor to Battelle Memorial Institute, under its prime contract with NIAID (contract HHSN272200200016I). NERCE/BEID, Boston, MA, provided a Career Development Fellowship to J.H.K. (grant A1057159). Agence Nationale de la Recherche supported V.E.V. (ANR-07-MIME-006-01).

We thank Gordon Ruthel (USAMRIID, Fort Detrick, Frederick, MD) for analyzing samples with the Discovery-1 microscope. We thank Reed F. Johnson and Mike Bray for reviewing the manuscript.

Opinions, interpretations, conclusions, and recommendations are those of the authors and are not necessarily endorsed by the U.S. Department of Defense, the U.S. Department of the Army, or the U.S. Department of Health and Human Services.

#### REFERENCES

- Aiken, C., J. Konner, N. R. Landau, M. E. Lenburg, and D. Trono. 1994. Nef induces CD4 endocytosis: requirement for a critical dileucine motif in the membrane-proximal CD4 cytoplasmic domain. *Cell* **76**:853–864.
- Barrette, R. W., et al. 2009. Discovery of swine as a host for the *Reston ebolavirus*. *Science* **325**:204–206.
- Barrientos, L. G., A. M. Martin, P. E. Rollin, and A. Sanchez. 2004. Disulfide bond assignment of the Ebola virus secreted glycoprotein SGP. *Biochem. Biophys. Res. Commun.* **323**:696–702.
- Casari, G., C. Sander, and A. Valencia. 1995. A method to predict functional residues in proteins. *Nat. Struct. Biol.* **2**:171–178.
- Chan, S. Y., R. F. Speck, M. C. Ma, and M. A. Goldsmith. 2000. Distinct mechanisms of entry by envelope glycoproteins of Marburg and Ebola (Zaire) viruses. *J. Virol.* **74**:4933–4937.
- Chandran, K., N. J. Sullivan, U. Felber, S. P. Whelan, and J. M. Cunningham. 2005. Endosomal proteolysis of the Ebola virus glycoprotein is necessary for infection. *Science* **308**:1643–1645.
- Dalgleish, A. G., et al. 1984. The CD4 (T4) antigen is an essential component of the receptor for the AIDS retrovirus. *Nature* **312**:763–767.
- Dube, D., et al. 2009. The primed ebolavirus glycoprotein (19-kilodalton GP<sub>1,2</sub>): sequence and residues critical for host cell binding. *J. Virol.* **83**:2883–2891.
- Dyson, H. J., and P. E. Wright. 2005. Intrinsically unstructured proteins and their functions. *Nat. Rev. Mol. Cell Biol.* **6**:197–208.
- el Mekki, A. A., and G. van der Groen. 1981. A comparison of indirect immunofluorescence and electron microscopy for the diagnosis of some haemorrhagic viruses in cell cultures. *J. Virol. Methods* **3**:61–69.
- Falzarano, D., et al. 2006. Structure-function analysis of the soluble glycoprotein, sGP, of Ebola virus. *ChemBioChem* **7**:1605–1611.
- Feldmann, H., V. E. Volchkov, V. A. Volchkova, U. Ströher, and H.-D. Klenk. 2001. Biosynthesis and role of filoviral glycoproteins. *J. Gen. Virol.* **82**:2839–2848.
- Gallaher, W. R. 1996. Similar structural models of the transmembrane proteins of Ebola and avian sarcoma viruses. *Cell* **85**:477–478.
- Geisbert, T. W., and P. B. Jahrling. 1995. Differentiation of filoviruses by electron microscopy. *Virus Res.* **39**:129–150.
- Huang, I. C., et al. 2008. Influenza A virus neuraminidase limits viral superinfection. *J. Virol.* **82**:4834–4843.
- Ito, H., S. Watanabe, A. Takada, and Y. Kawaoka. 2001. Ebola virus glycoprotein: proteolytic processing, acylation, cell tropism, and detection of neutralizing antibodies. *J. Virol.* **75**:1576–1580.
- Ito, H. S., S. Watanabe, A. Sanchez, M. A. Whitt, and Y. Kawaoka. 1999. Mutational analysis of the putative fusion domain of Ebola virus glycoprotein. *J. Virol.* **73**:8907–8912.
- Klatzmann, D., et al. 1984. T-lymphocyte T4 molecule behaves as the receptor for human retrovirus LAV. *Nature* **312**:767–768.
- Kuhn, J. H. 2008. Filoviruses—a compendium of 40 years of epidemiological, clinical, and laboratory studies. *Arch. Virol. Suppl.* **20**:13–360.
- Kuhn, J. H., et al. 2010. Proposal for a revised taxonomy of the family *Filoviridae*: classification, names of taxa and viruses, and virus abbreviations. *Arch. Virol.* **155**:2083–2103.
- Kuhn, J. H., et al. 2006. Conserved receptor-binding domains of Lake Victoria Marburg virus and Zaire Ebola virus bind a common receptor. *J. Biol. Chem.* **281**:15951–15958.
- Lama, J., A. Mangasarian, and D. Trono. 1999. Cell-surface expression of CD4 reduces HIV-1 infectivity by blocking Env incorporation in a Nef- and Vpu-inhibitable manner. *Curr. Biol.* **17**:622–631.
- Lee, J. E., et al. 2008. Structure of the Ebola virus glycoprotein bound to an antibody from a human survivor. *Nature* **454**:177–182.
- Leroy, E. M., et al. 2005. Fruit bats as reservoirs of Ebola virus. *Nature* **438**:575–576.
- Li, W., et al. 2003. Angiotensin-converting enzyme 2 is a functional receptor for the SARS coronavirus. *Nature* **426**:450–454.
- Livingstone, C. D., and G. J. Barton. 1993. Protein sequence alignments: a strategy for the hierarchical analysis of residue conservation. *Comput. Appl. Biosci.* **9**:745–756.
- Mangasarian, A., et al. 1997. The HIV-1 Nef protein acts as a connector with sorting pathways in the Golgi and at the plasma membrane. *Immunity* **6**:67–77.
- Manicassamy, B., and L. Rong. 2009. Expression of Ebolavirus glycoprotein on the target cells enhances viral entry. *Virol. J.* **6**:75.
- Manicassamy, B., et al. 2007. Characterization of Marburg virus glycoprotein in viral entry. *Virology* **358**:79–88.
- Mar'ankova, R. F., S. E. Glušakova, E. V. Ryzik, and I. S. Lukašević. 1993. Marburg virus penetration into eukaryotic cells. *Vopr. Virusol.* **38**:74–76.
- Maruyama, T., et al. 1999. Recombinant human monoclonal antibodies to Ebola virus. *J. Infect. Dis.* **179**(Suppl. 1):S235–S239.
- Maruyama, T., et al. 1999. Ebola virus can be effectively neutralized by antibody produced in natural human infection. *J. Virol.* **73**:6024–6030.
- Mehedi, M., et al. 2011. A new Ebola virus nonstructural glycoprotein expressed through RNA editing. *J. Virol.* **85**:5406–5414.
- Morikawa, S., M. Saijo, and I. Kurane. 2007. Current knowledge on lower virulence of Reston Ebola virus. *Comp. Immunol. Microbiol. Infect. Dis.* **30**:391–398.
- Radoshitzky, S. R., et al. 2007. Transferrin receptor 1 is a cellular receptor for New World haemorrhagic fever arenaviruses. *Nature* **446**:92–96.
- Rancurel, C., M. Khosravi, K. A. Dunker, P. R. Romero, and D. Karlin. 2009. Overlapping genes produce proteins with unusual sequence properties and offer insight into *de novo* protein creation. *J. Virol.* **83**:10719–10736.
- Ruiz-Argüello, M. B., F. M. Goñi, F. B. Pereira, and J. L. Nieva. 1998. Phosphatidylinositol-dependent membrane fusion Induced by a putative fusogenic sequence of Ebola virus. *J. Virol.* **72**:1775–1781.
- Sanchez, A. 2007. Analysis of filovirus entry into vero e6 cells, using inhibitors of endocytosis, endosomal acidification, structural integrity, and cathepsin (B and L) activity. *J. Infect. Dis.* **196**(Suppl. 2):S251–S258.
- Sanchez, A., M. P. Kiley, B. P. Holloway, and D. D. Auperin. 1993. Sequence analysis of the Ebola virus genome: organization, genetic elements, and comparison with the genome of Marburg virus. *Virus Res.* **29**:215–240.
- Sanchez, A., S. G. Trappier, B. W. J. Mahy, C. J. Peters, and S. T. Nichol.

1996. The virion glycoproteins of Ebola viruses are encoded in two reading frames and are expressed through transcriptional editing. *Proc. Natl. Acad. Sci. U. S. A.* **93**:3602–3607.
41. **Schorberg, K., et al.** 2006. Role of endosomal cathepsins in entry mediated by the Ebola virus glycoprotein. *J. Virol.* **80**:4174–4178.
42. **Schorberg, K. L., et al.** 2009.  $\alpha_5\beta_1$ -Integrin controls ebolavirus entry by regulating endosomal cathepsins. *Proc. Natl. Acad. Sci. U. S. A.* **106**:8003–8008.
43. **Takada, A., et al.** 1997. A system for functional analysis of Ebola virus glycoprotein. *Proc. Natl. Acad. Sci. U. S. A.* **94**:14764–14769.
44. **Tompa, P., and M. Fuxreiter.** 2008. Fuzzy complexes: polymorphism and structural disorder in protein-protein interactions. *Trends Biochem. Sci.* **33**:2–8.
45. **Towner, J. S., et al.** 2009. Isolation of genetically diverse Marburg viruses from Egyptian fruit bats. *PLoS Pathog.* **5**:e1000536.
46. **Towner, J. S., et al.** 2008. Newly discovered ebola virus associated with hemorrhagic fever outbreak in Uganda. *PLoS Pathog.* **4**:e1000212.
47. **van der Groen, G.** 1978. Growth of Lassa and Ebola viruses in different cell lines, p. 255–260. *In* S. R. Pattyn (ed.), *Ebola virus haemorrhagic fever*. Elsevier/North-Holland Biomedical Press, Amsterdam, The Netherlands.
48. **Volchkov, V. E., et al.** 1995. GP mRNA of Ebola virus is edited by the Ebola virus polymerase and by T7 and vaccinia virus polymerase. *Virology* **214**:421–430.
49. **Volchkov, V. E., H. Feldmann, V. E. Volchkova, and H.-D. Klenk.** 1998. Processing of the Ebola virus glycoprotein by the proprotein convertase furin. *Proc. Natl. Acad. Sci. U. S. A.* **95**:5762–5767.
50. **Volchkov, V. E., V. A. Volchkova, O. Dolnik, H. Feldmann, and H.-D. Klenk.** 2005. Polymorphism of filovirus glycoproteins, p. 359–381. *In* P. Roy (ed.), *Virus structure and assembly*. Elsevier/Academic Press, San Diego, CA.
51. **Volchkov, V. E., et al.** 2000. Proteolytic processing of Marburg virus glycoprotein. *Virology* **268**:1–6.
52. **Volchkova, V. A., O. Dolnik, M. J. Martinez, O. Reynard, and V. E. Volchkov.** Genomic RNA editing and its impact on Ebola virus adaptation during serial passages in cell culture and infection of guinea pigs. *J. Infect. Dis.*, in press.
53. **Volchkova, V. A., H. Feldmann, H.-D. Klenk, and V. E. Volchkov.** 1998. The nonstructural small glycoprotein sGP of Ebola virus is secreted as an antiparallel-oriented homodimer. *Virology* **250**:408–414.
54. **Volchkova, V. A., H.-D. Klenk, and V. E. Volchkov.** 1999. Delta-peptide is the carboxy-terminal cleavage fragment of the nonstructural small glycoprotein sGP of Ebola virus. *Virology* **265**:164–171.
55. **Wagner, R., M. Matrosovich, and H.-D. Klenk.** 2002. Functional balance between haemagglutinin and neuraminidase in influenza virus infections. *Rev. Med. Virol.* **12**:159–166.
56. **Wahl-Jensen, V., et al.** 2005. Effects of Ebola virus glycoproteins on endothelial cell activation and barrier function. *J. Virol.* **79**:10442–10450.
57. **Watanabe, S., et al.** 2000. Functional importance of the coiled-coil of the Ebola virus glycoprotein. *J. Virol.* **74**:10194–10201.
58. **Willey, R. L., F. Maldarelli, M. A. Martin, and K. Strebel.** 1992. Human immunodeficiency virus type 1 Vpu protein regulates the formation of intracellular gp160-CD4 complexes. *J. Virol.* **66**:226–234.
59. **Wong, S. K., W. Li, M. J. Moore, H. Choe, and M. Farzan.** 2004. A 193-amino acid fragment of the SARS coronavirus S protein efficiently binds angiotensin-converting enzyme 2. *J. Biol. Chem.* **279**:3197–3201.
60. **Wool-Lewis, R. J., and P. Bates.** 1998. Characterization of Ebola virus entry by using pseudotyped viruses: identification of receptor-deficient cell lines. *J. Virol.* **72**:3155–3160.